NASA Contractor Report 179430

Spectral Contents Readout of Birefringent Sensors

Alex S. Redner and Arkady S. Voloshin

(NASA-CR-179430) SPECTRAL CONTENTS READOUT OF BIREFRINGENT SENSORS Final Report (Strainoptic Technologies) 40 p CSCL 20K

N88-20673

Unclas
G3/39 0136062

Contract NAS 2-12351
April 1988

National Aeronautics and
Space Administration

NASA Contractor Report 179430

Spectral Contents Readout of Birefringent Sensors

Alex S. Redner and Arkady S. Voloshin
Strainoptic Technologies, Inc., P.O. Box 177, Norristown, Pennsylvania 19404

Prepared for
Ames Research Center
Dryden Flight Research Facility
Edwards, California
Under Contract NAS 2-12351
1988

National Aeronautics and
Space Administration
Ames Research Center
Dryden Flight Research Facility
Edwards, California 93523-5000

CONTENTS

		Page
1.	SUMMARY	2
2.	RESEARCH OBJECTIVES	3
2.1	Introduction - Fundamentals	3
2.2	Objectives	7
3.	RESEARCH WORK AND RESULTS	9
3.1	Design and Construction of the SPECTRAL-CONTENTS ANALYSIS Polarimeter	9
3.2	Selection of Algorithms & Programming of the Data-Acquisition Microcomputer	13
3.3	Evaluation of Materials	23
3.4	Analysis of the Quarter-Wave Plate Behavior in a White Light Polariscope	24
3.5	Problems Associated with the Selection of the Spectral Range, and Choice of the Photodiode Spacing	26
3.6	Use of Fiber-Optic Cables for Data Acquisition	27
3.7	System Evaluation	30
4.	SUMMARY OF THE RESULTS	31
5.	ESTIMATES OF THE TECHNICAL FEASIBILITY	31
5.1	Instrumentation Development	31
5.2	Material Characteristics	32
5.3	Precision Evaluation	32
5.4	Potential Applications	32
6.	CONCLUSIONS AND RECOMMENDATIONS	33
-	References	35
-	Appendix	36

1. SUMMARY

Purpose of the Research

The objective of the research work performed was to establish the feasibility of using SPECTRAL CONTENTS ANALYSIS to measure accurately, strains and retardation in BIREFRINGENT SENSORS, and more generally, on transparent materials.

Description of the Work Carried Out

Transparent materials subjected to strain develop birefringence. A sequence of colors can be observed when a stressed material is placed between polarizers. The SPECTRAL CONTENTS method uses a spectral analyzer that divides the light into several beams carrying narrow wavelengths and measuring light intensity at discrete intervals. The analysis of this information by a microcomputer permits the identification of the strain in the sensor. A special purpose spectral anlayzer capable of performing this task was designed, produced and interfaced to a microcomputer. Equations and programs were developed for the analysis of the data received by the microcomputer. Chromatic characteristics of three sensor materials and of the polarimeter were measured and the results of analysis incorporated in the data handling procedures.

The system was made operational and the measurements obtained by the system were compared to the measurements obtained using traditional methods.

Results

As result, it was found that the proposed concept is feasible, simple to implement, capable of precision that exceeds the presently available methods of measuring the birefringence. The instrument system proved workable and the algorithms developed for data handling proved capable to operate the microcomputer efficiently, interpret accurately the measured light intensity and translate it into birefringence and strain.

Applications

The potential applications include:

-Automation of Photoelastic Stress Analysis

-Readout of birefringent sensors, including fiber-optic strain gages and transducers using birefringent sensors.

-High temperature birefringent sensors, with data transmission on fiber-optic cables.

-Process Control and QC of glass and plastic products.

2. RESEARCH OBJECTIVES

2.1. Introduction - Fundamentals

Transparent materials subjected to stress become birefringent. A polarized beam of light crossing a stressed item splits into two waves, propagating at two different speeds and vibrating in the plane of principal stresses (Figure 1). After crossing the stressed material - the two beams emerge out of phase. The distance δ between these beams is proportional to the difference in velocities $n_1 - n_2$.

$$\delta = (n_1 - n_2)t \qquad (1)$$

The BIREFRINGENCE $n_1 - n_2$ is proportional to the difference of principal strains $(\varepsilon_1 - \varepsilon_2)$ and within elastic limits, also to the difference of principal stresses.

$$n_1 - n_2 = k(\varepsilon_1 - \varepsilon_2) = C(\sigma_1 - \sigma_2) \qquad (2)$$

and $$\delta = (n_1 - n_2)t = tk(\varepsilon_1 - \varepsilon_2) = tC(\sigma_1 - \sigma_2)$$

where k is the strain optic material constant , t is the thickness, and C is the Brewster constant.

Both k and C are material properties and can be obtained by calibration.

Measurements of the retardation δ can yield the strain or stress. Combining (1) and (2) above, yields:

$$\sigma_1 - \sigma_2 = \frac{\delta}{t \cdot C} \quad \text{or} \quad \varepsilon_1 - \varepsilon_2 = \frac{\delta}{kt} \qquad (3)$$

2.1.1. MEASUREMENTS OF BIREFRINGENCE

Using this concept, stresses can be measured in practical applications, including:

-EXPERIMENTAL STRESS ANALYSIS OF PHOTOELASTIC MODELS

-MEASURING SURFACE STRESSES ON STRUCTURES USING PHOTOELASTIC COATINGS

-INSPECTION OF GLASS AND PLASTIC PRODUCTS

-QUALITY CONTROL OF STRENGTHENED GLASS

-MEASURING STRAIN IN BIREFRINGENT SENSORS

Unfortunately, presently available methods for measuring the retardation δ are cumbersom and difficult to practice. The measured item is placed between polarizing elements (Figure 1). The light intensity emerging from a system including quarter-wave plate can be described as follows:

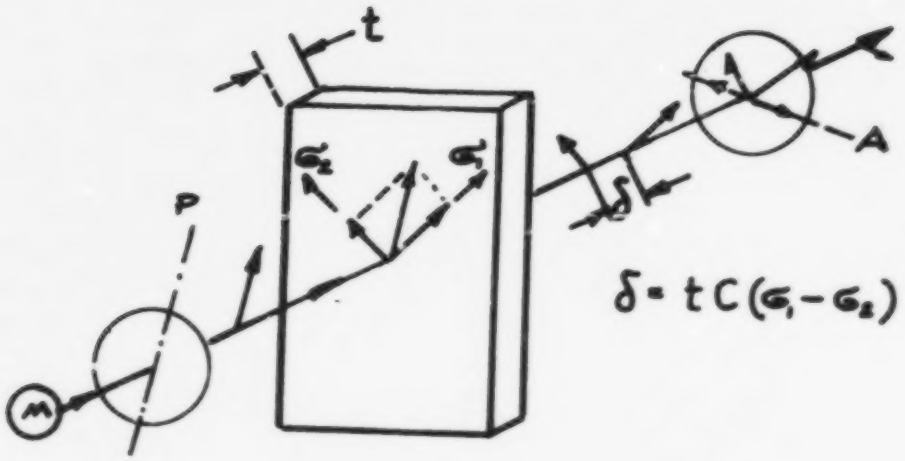

S Light Source
P,A Polarizers
$Q_1 Q_2$ Quarter Wave-Plates
σ_1 σ_2 Principal Stresses

Light Field: $I = I_0 \cos^2 \frac{\pi \delta}{\lambda}$

Dark Field: $I = I_0 \sin^2 \frac{\pi \delta}{\lambda}$

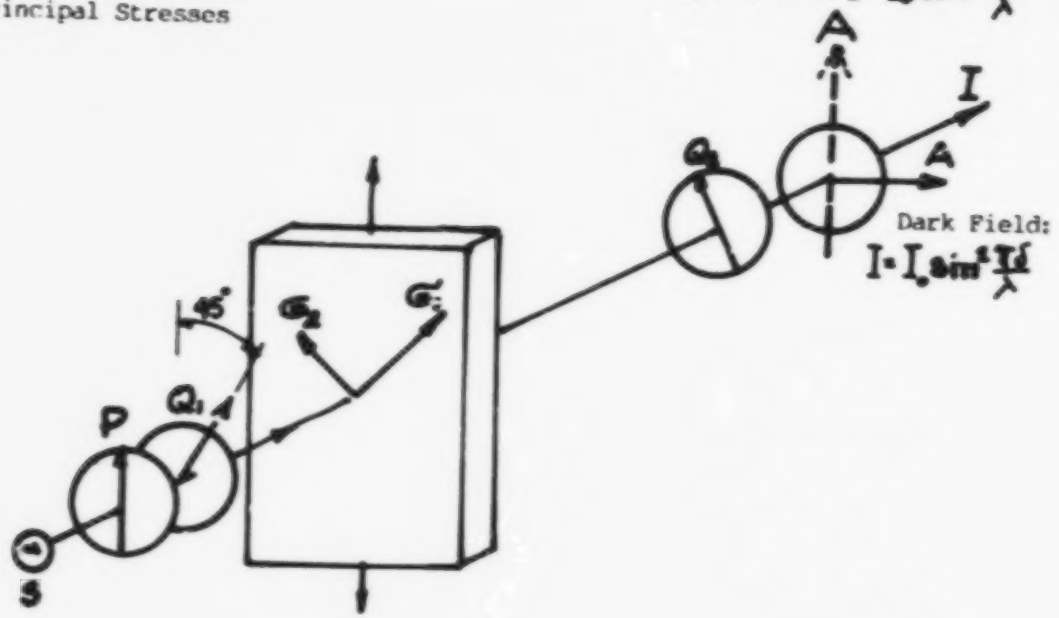

FIGURE 1. POLARISCOPE SET-UP FOR MEASUREMENTS OF BIREFRINGENCE.

Circular Polariscope DARK FIELD $I = I_o \text{Sin}^2 \frac{\pi\delta}{\lambda}$ (4)

LIGHT FIELD $I = I_o \text{Cos}^2 \frac{\pi\delta}{\lambda}$ (5)

In monochromatic light dark fringes are obsrved when I = 0 or

$$\delta = N\lambda \quad (N = 0, 1, 2.....) \tag{6}$$

N is an arbitrary integer, that cannot be positively assessed, or measured.

In white light, the pattern of fringes δ = Constant appears in color. Using a compensator (1)(2), one can measure δ visually. These measurements are requiring a highly skilled operator, and the precision is affected by the operator's judgment and experience.

These difficulties contributed to the decrease in popularity of the photoelastic stress analysis and to the difficulties faced by the glass and plastic industry in their attempts to implement quality control procedure and process controls based on stress measurements.

More recently, fiber-optic sensors appeared as a very desirable form of a sensor. A birefringent fiber-optic sensor (or gage) offer several significant advantages:

-Capability of a non-contacting readout

-Immunity to electrical or magnetic noise

-Data transmission by fiber-optic cables

-Capability of operating at elevated temperature

-Environmental ruggedness

Presently existing methods are not suitable for measuring birefringence in these sensors.

The recently proposed SPECTRAL CONTENTS ANALYSIS method of measuring δ (SCA) (3) eliminates most of the difficulties and limitations of the visual techniques. This method can be used in stress anlaysis, glass and plastic inspection and also offers an ideal solution to the problem of measuring the birefringence and strain in fiber-optic sensors.

The concept of the Spectral Contents Analysis method is simple. A stressed member placed in a polariscope (Figure 2) is considered acting as a modulator of the spectral transmittance. Each state of stress produces a typical visible color (or spectral signature) described by the equations (4) and (5) above.

Figure 3 shows some typical "Signatures" that should be theorectically observed.

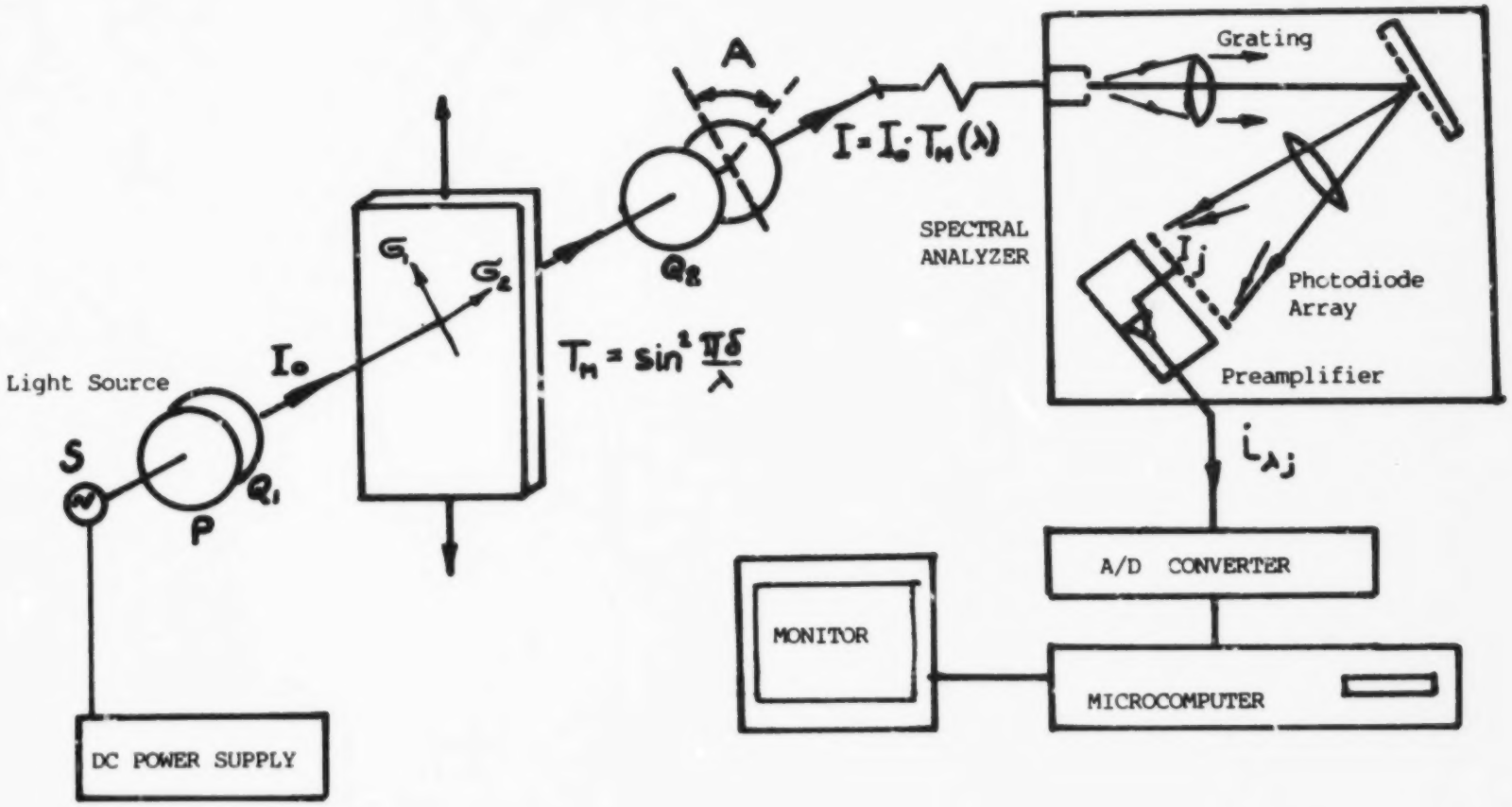

FIGURE 2. SPECTRAL CONTENTS ANALYSIS METHOD. SYSTEM SCHEMATIC FOR MEASUREMENTS OF RETARDATION

To acquire the "Spectral Contents" of the transmitted light, the light that crossed the stressed member is divided using a diffraction grating into narrow wavelength components and projected on a photodiode array (Figure 2).

Each photodiode current i_j is proportional to the intensity I_j of light carried by λ_j:

$$I_j = I_{oj} \times \text{Sin}^2 \frac{\pi\delta}{\lambda_j} = S(\lambda_j) \cdot T_M \qquad (7)$$

where: I_{oj} is a calibration term describing the source and the overall system transmittance.

and: $T_M = \text{Sin}^2 \frac{\pi\delta}{\lambda_j}$ is the contribution of the birefringent element to the spectral transmittance.

The currents i_j provides many points of the spectral signature. To retrieve δ from the signature - it is necessary to "fit" a $\text{Sin}^2 \frac{\pi\delta}{\lambda}$ curve to these points (Figure 4). The best "fitting" process is one of the topics of this research program and is more thoroughly described below.

2.2. Objectives

The objective of the research work performed under this contract was to establish the FEASIBILITY of measuring the Birefringence and Stresses in transparent materials using the SPECTRAL CONTENTS ANALYSIS.

Since the method until now existed only in a form of a concept, the work on this feasibility study had to include the construction of a special test apparatus shown schematically on the Figure 2. The overall objectives were:

2.2.1. Build a SPECTRAL-CONTENTS ANLAYSIS POLARISCOPE suitable to measure the retardation δ, including in the construction sufficient flexibility to permit variation of the parameters that needed to be evaluated.

2.2.2. Develop a program, capable of receiving the light intensity measured at several discrete wavelengths and calculating from this information the retardation and birefringence.

2.2.3. Assessing the suitability of a material for the use as a sensor, analyzed by spectral contents method.

2.2.4. Analysis of element(s) that are strongly wavelength-dependent, (such as a quarter-wave plate) and their influence on the system potential precision.

2.2.5. Selection of a practical region of the spectrum for the implementation of this method.

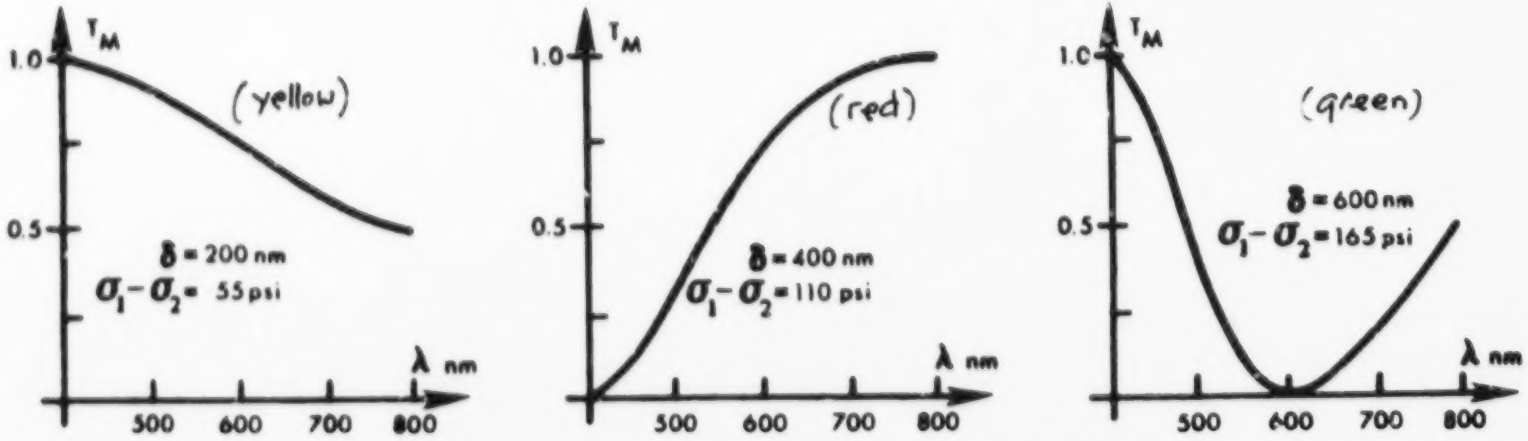

FIGURE 3. SPECTRAL SIGNATURE OF A STRESSED SENSOR
Material: Polycarbonate, ½ in. thick.

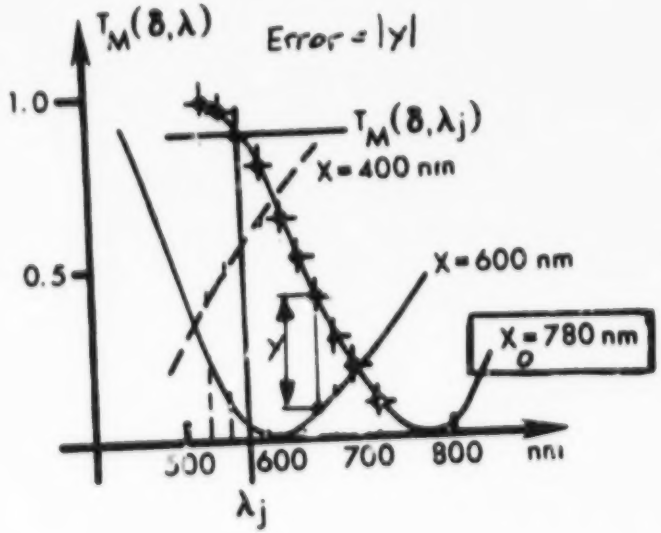

FIGURE 4. Fitting of a curve $\sin^2 \frac{\pi d}{\lambda}$ to a set of measured values of T_M

2.2.6. Evaluation of chromatic problems generated when a fiber-optic cable is incorporated in the system.

2.2.7. Evaluation of sensor-material suitability and analysis of materials characteristic/property.

2.2.8. Evaluation of factors affecting the system stability.

2.2.9. SYSTEM PERFORMANCE - Evaluation of the Feasibility of the SPECTRAL CONTENTS ANALYSIS.

3. RESEARCH WORK CARRIED AND RESULTS OBTAINED

3.1 Design and Contruction of the Spectral-Contents Analysis Polarimeter

The test-apparatus is shown schematically Figure 2. The completed system designed and produced is shown on the Figure 7 and includes:

3.1.1. Light Source - A 50 watt 30 volt regulated power supply was used to supply a regulated DC voltage to a quartz-halogen lamp, equipped with a mirror, to project the image of the filament on an aperture, producing a conical beam, or to inject the light into the fiber-optic cable, used for illumination.

3.1.2. Polarimeter

In this experimental model, both the illuminating and receiving cells included a rotating polarizer, and a scale permitting any desired angular position of the polarizer (see Figure 5). A rotatable quarter-wave plate was designed with notches, for easy positioning at 45° to polarizer axes.

3.1.3. Spectral Analyzer

The spectral analyzer was designed to permit selection of parameters that were investigated. It consisted of an entrance slit, a collimating set of identical lenses, to project the received light on a diffraction grating and then back on the photodiode array, yielding the dispersion of wavelength compatible with the spacing of the photodiode. Figure 7 shows the completed system. The Spectral analyzer is shown Figure 6.

The PHOTODIODE ARRAY consisted of 32 photodiodes, each one 1.3mm x 0.585mm wide, with 0.635mm spacing center-to-center, mounted in a 40 pin DIP socket.

The output of each photodiode was connected to a preamplifier, mounted a board near the photodiode socket, to insure a very short lead between the photodiode pin and the preamp. IC to minimize the noise pick-up. The schematic of the preamplifier circuit is shown Figure 8. The preamplifier output was adjusted, to show the same current at equal illumination, to better illustrate the spectral response of the system.

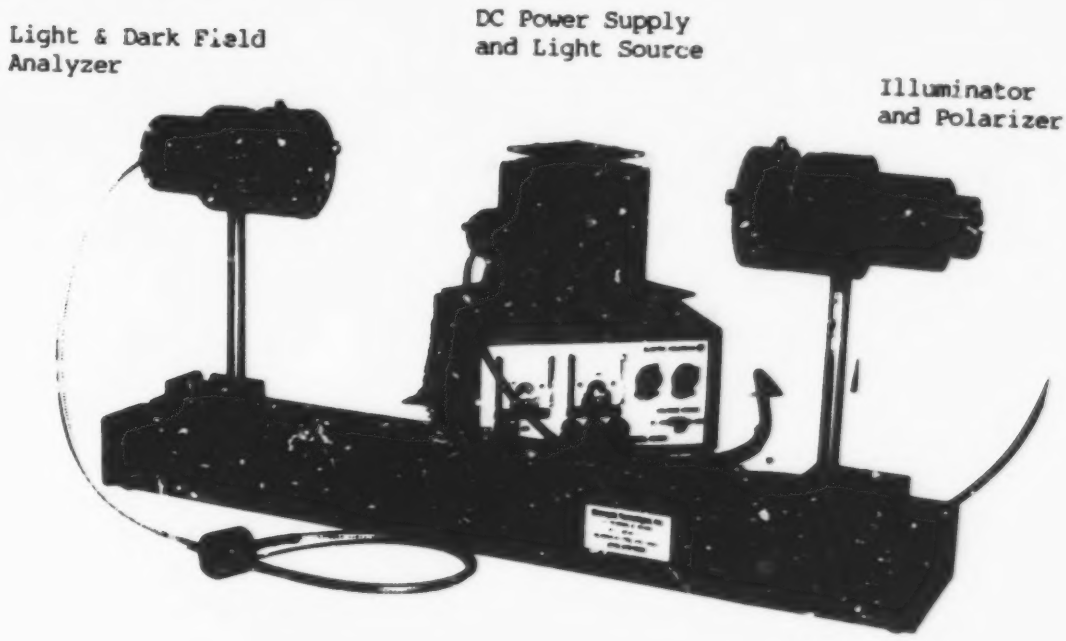

FIGURE 5. POLARIMETER FOR SPECTRAL-CONTENTS ANALYSIS R&D.

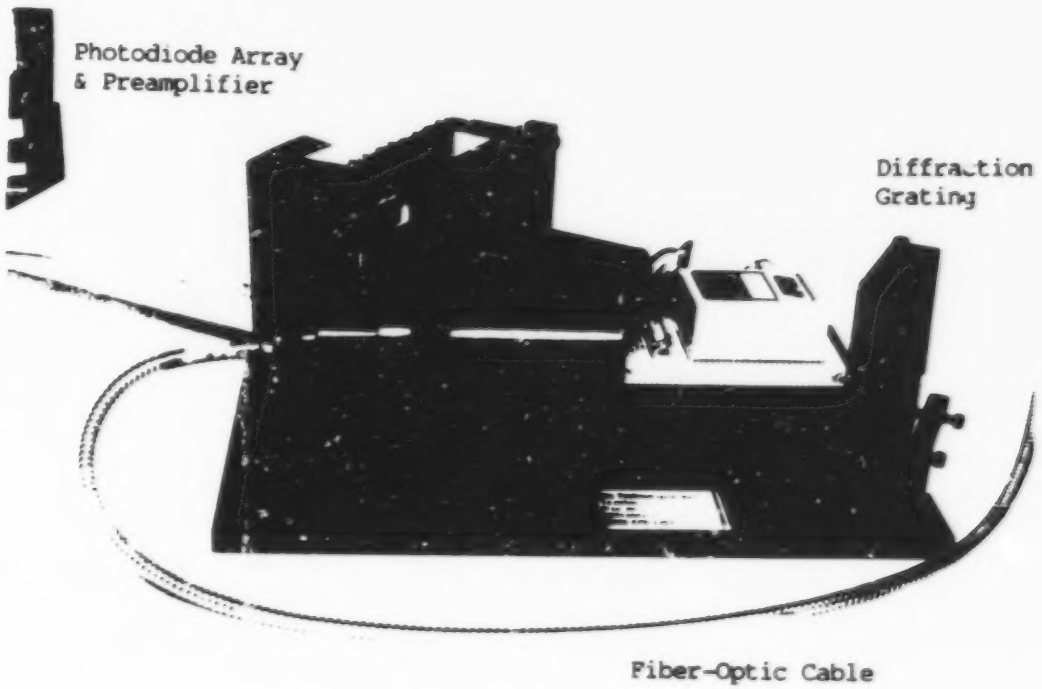

FIGURE 6. SPECTRAL ANALYZER.

ORIGINAL PAGE IS
OF POOR QUALITY

ORIGINAL PAGE IS
OF POOR QUALITY

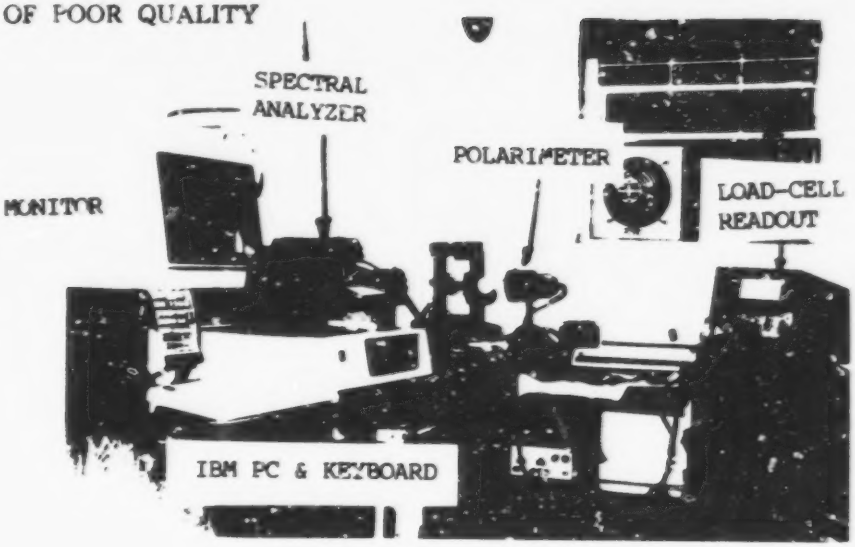

COMPLETED SYSTEM IN OPERATION

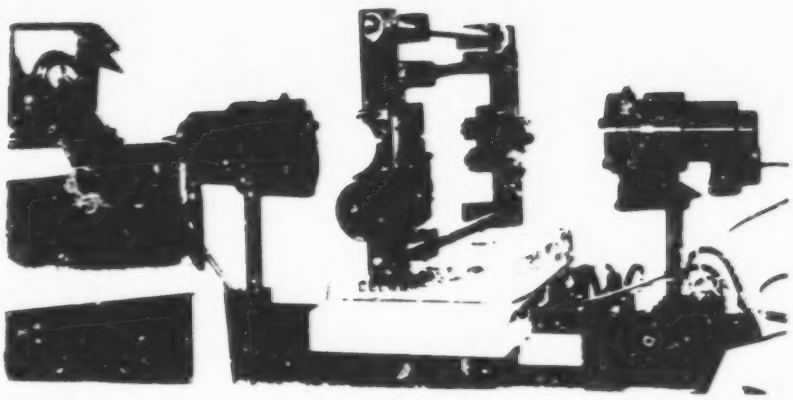

TENSILE SPECIMEN IN EVALUATION

FIGURE 7

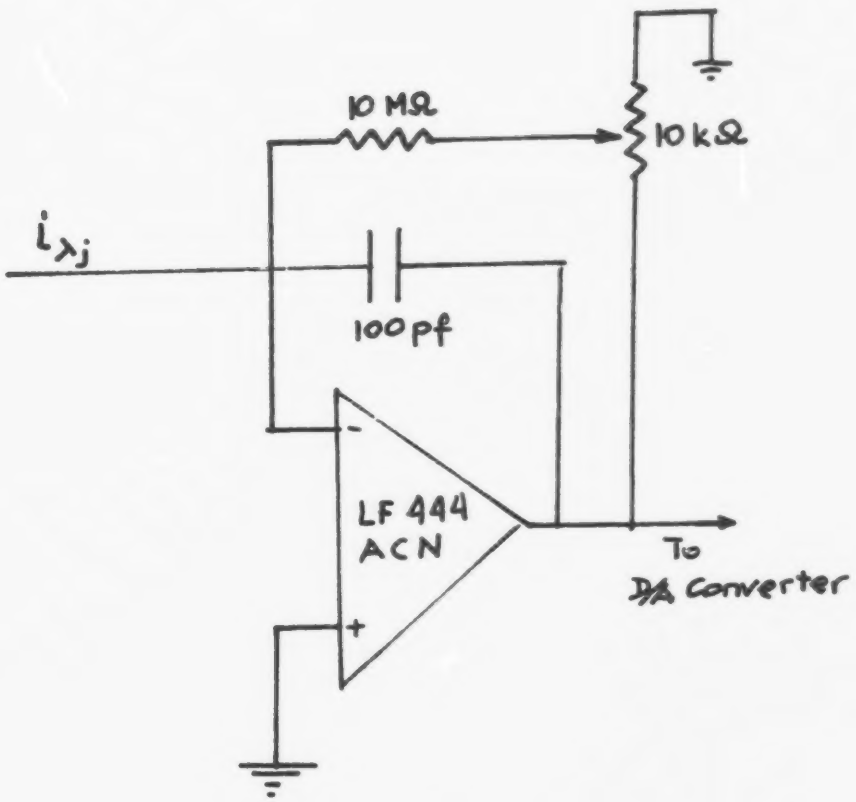

PHOTODIODE PREAMPLIFIER

FIGURE 8

3.1.4. A/D Converter

In order to interface the photodiode outputs to the PC used for analysis of data and curve-fitting process, an analogue-to-digital converted, compatible with the PC was installed. For this work, a METRABYTE model DASH 16 was acquired and installed, in one of the expansion slots of the PC.

3.1.5. Microcomputer

For data-acquisition, fitting function and operation of the system an IBM-XT microcomputer was used with an AMTEK monochrome monitor for display of the desired information.

3.1.6. Results

The initial set-up and calibration was required to ascertain the wavelength received by each photodiode of the array. This calibration was accomplished using a series of interferential filters and measuring the transmitted light intensity. After completion of this initial calibration, the system performed throughout the program duration without any problem.

3.2. Selection of Algorithms and Programming of the Data-Acquisition Microcomputer

3.2.1. Problem to be Solved

The equations (4) and (5) above provide an idealized light intensity I, transmitted by the system, as function of the measured retardation δ.

$$I/I_0 = \mathrm{Sin}^2 \frac{\pi\delta}{\lambda} = T_M(\delta,\lambda)$$

For a monochromatic light, of wavelength λ, the solution has multiple roots:

$$\frac{\pi\delta}{\lambda} = \pm \mathrm{Sin}^{-1} \sqrt{T_M} + n\pi$$

where n is an integer. Since n is unknown, the monochromatic light cannot yield a solution for δ.

To obtain a solution, SEVERAL wavelengths must be employed. In the system evaluated here, 16 wavelengths were available for measurements. The system was tested with 6, 8 and 16 photodiodes, to assess the minimal number needed to extract δ from the measured light intensity.

-As illustrated in Figure 4, the SPECTRAL-CONTENTS ANALYSIS is based on matching the measured values of T_M to a theoretical spectral distribution. To accomplish this objective, the expression of the transmitted light intensity must be first expanded, to include the characteristics of a real system.

3.2.1.1. Influence of the Quarter-Wave Plate

The quarter-wave plate provides a $\frac{1}{4}$ wavelength retardation for one value of λ_o only. For other wavelength, the transmitted light intensity must be corrected by a factor (derived in 3. 4 below):

$$T_M = \text{Sin}^2 \frac{\pi\delta}{\lambda_j} (1-\text{Sin}^2\ 2\alpha\ \text{Sin}^2 e_j) \qquad (8)$$

where α is the angle between the quarter-wave plate and the direction of stresses

and e is the quarter-wave plate error for a radiation of wavelength λ_j expressed by:

$$e = \frac{\pi}{2} (\frac{\lambda o}{\lambda_j} - 1) \qquad (9)$$

In some applications the angle α is known and the correction can be easily implemented. In other instances, a middle-value of 0.5 can be used, to minimize the error in the term $\sin^2 2\alpha$, when its exact value is not known.

3.2.1.2. Influence of the Photodiode Size

The physical dimensions of the individual elements of the photodiode array, combined with the slit aperture, the frequency of the grating and with the lens focal lengths determines the width of the spectrum $\Delta\lambda$ observed by each photodiode (from λ_{j1} to λ_{je}). As result, each photodiode integrates over its own area:

$$I(\delta\lambda_j) = \int_{\lambda j_1}^{\lambda j_2} I(\lambda) d\lambda \qquad (10)$$

3.2.1.3. Efficiency of Polarizers

The polarizer employed (POLAROID Corp. Model HN32) are not very efficient, mostly when used at the blue and red end of the spectrum. The light intensity measured at different wavelengths "j" in DARK FIELD (crossed P and A) becomes $DF(\delta)$ and must be included, in the transmittance evaluation.

3.2.1.4. Source Characteristics

The term I_{oj} includes the spectral characteristics of the source and transmittance of all the passive components. I_{oj} requires an "update" since the intensity of the light source changes with time, as the light source "burns".

3.2.1.5. Dispersion Correction

In all above considerations it was assumed that δ is a constant, function of stresses only. In some materials the chromatic dispersion of birefringence is not negligible and the dispersion-corrected expression should be introduced, as derived in 3.3.2. below:

$$T(\delta,\lambda_j) = \sin^2 \frac{\pi\delta}{\lambda_j} \cdot \frac{C(\lambda_j)}{C(\lambda_o)} \qquad (11)$$

3.2.1.6. Combining all the influences and corrections shown above, the final expression of the transmitted light intensity becomes:

$$I(\delta)_j = \int_{\lambda_{1j}}^{\lambda_{2j}} I_o(\lambda) \sin^2\left(\frac{\pi\delta}{\lambda} \cdot \frac{Cj}{Co}\right) X \left(1-\sin^2 2\alpha \sin^2 e\right) d\lambda + DF(j) \qquad (12)$$

Replacing $I_o(\lambda)$ by its mean value and assuming $\sin^2 2\alpha = 0.5$ yields a simplified form.

$$I(\delta)_j = I_{oj} \int_{\lambda_{1j}}^{\lambda_{2j}} (1-0.5\sin^2 e)\sin^2\left(\frac{\pi\delta}{\lambda}\right) d\lambda + DF(j) \qquad (13)$$

Here for simplicity, Cj/Co was assumed to be 1. (This material characteristic can be easily stored for use when required).

The expressions (12) and (13) above were used in the final evaluation and programming.

3.2.2. Calibration of the System

Several techniques for system calibration and updating can be devised. One of the possibilities is the use of both dark and light field circular polariscopes. First, data is acquired by all 16 diodes in a dark field setup with unloaded specimen in the polariscope, thus 16 values for evaluation of DF(j), are recorded. Then analyzer is rotated by 90° and a second set of information is acquired:

$$I_j(\delta) = I_o(j) \int_{\lambda_{1j}}^{\lambda_{2j}} \cos^2\left(\frac{\pi\delta}{\lambda}\right) * (1-0.5 * \sin^2 e)\, d\lambda + DF(j) \qquad (14)$$

The term $P = 1 - 0.5 \sin^2 e$ changes relatively little and is monotonic within the range of each diode, for example:

$P = 0.9173$ for $\lambda = 450$nm

and

$P = 0.9462$ for $\lambda = 470$nm

which was the range of the first diode of the array. The change here is about 3%. For all other diodes the change is smaller, and it drops to below 0.6% for the diode in the 740–760nm range. The average value of P thus can be easily evaluated for each diode. Using this information and data for the light intensity acquired by each diode in dark and light field setup, the values of $I_o(j)$ and DF(j) will be recorded and used later for evaluation of the retardation δ.

Similar procedure can be used during regular updates of the system, the frequency of these updates are dependent on the particular application.

3.2.3. Methods for extracting the Retardation δ from the Measured Light Intensitites

3.2.3.1. Error-Function Minimization Approach

After performing the calibration procedure and evaluating the average value of the P - term for each diode, equation (14) can be rewritten.

$$I_j(\delta) = I_{oj} \sum_{\lambda_{1j}}^{\lambda_{2j}} P(j) \, \mathrm{Sin}^2 \frac{\pi\delta}{\lambda} \Delta\lambda + DF(j) \qquad (15)$$

where λ_{j1} - represents the lower boundary for a diode "j"

λ_{j2} - represents the upper boundary for a diode "j"

$\Delta\lambda$ - is the frequency increment for a diode "j"

P(j) - is the mean value for $(1 - 0.5 \, \mathrm{Sin}^2 e)$ of a diode "j"

Value of $I_j(\delta)$ can be calculated for each possible retardation δ within the considered range, and compared to the actually measured value I_j^m. Given a set of n data points I_j^m within the range of measurements there is only one value of δ that satisfies for EACH photodiode j the relation:

$$I_j(\delta) - I_j^m = 0 \qquad (16)$$

To solve these n equations, the error-summation approach can be used. The search is made for value of δ that will minimize the error function $E(\delta)$. (see figure 10)

$$E(\delta) = \sum_{j=1}^{n} (I_j(\delta) - I_j^m) = \text{minimum} \qquad (17)$$

Equation 17 is solved by a simple search over the range of possible retardations from 0 to 5000nm in 10nm steps.

The range (5000nm) and step (10nm) can be selected arbitrarily, in accordance with the range and the need of resolution of the results that are needed. It is possible to store an array of calculated $I_j(\delta)$ for any number n of photodiodes and any increment of δ. The search for the solution of equation (17) can be considerably accelerated when:

a) The selected range decreases

b) The number of photodiodes decreases

c) The step of the search increases

In practice, a coarse search in steps of 50nm proved acceptable, with the final search around the approximate value proceeding in smaller steps, or using a linear approximation.

3.2.3.2. Data Base Search Approach

As an alternative approach for extracting the retardation value from measured spectral content of the signal, the data base search was tested. During initialization of the system, the present value of retardation in a specimen can be achieved by a controlled loading. The procedure of the data base creation was to apply known load, which results in the known retardation, and acquire light intensity by all photodiodes (maximum number 16) and store it in an array 16 elements wide. This loading procedure continued until an array of 200 X 16 was built and permanently stored on a disk.

To extract value of retardation during actual test, the acquired information (16 photodiode) was compared by each of the 200 columns in the data base and difference between actual reading and corresponding position in the data base was calculated and compared to the present limit. If the difference was less than the limit, a value of 1 was assigned to the flag, otherwise - flag was set to zero. This procedure is repeated for each photodiode and all values of flag were added.

After going through all columns, 200 flags were calculated. Their values were ranging from 0 to 16. The flag with highest reading denotes the position of the solution. In case of more than two flags giving the same maximum value, the preset limit was halted and procedure was repeated.

3.2.3.3. The Newton-Raphson Approach

Use of the Newton-Raphson approach for extraction of the retardation was suggested by Sanford (6). To account for experimental errors and some systematic errors the finite form of the equation (12) was modified to include additional parameters responsible for constant shift and rotation of the spectral response plot. However, some difficulties were encountered and two separate techniques were used for extracting of retardation lower than 2π and higher than 2π.

Here, the problem was approached as follows: The light intensity as acquired by each diode is presented as in eq. (15) with additional unknown scale factor β, which should take care of some minute changes in the calibration parameter $I_o(j)$ because of light source and amplifiers instability. Let us create a function $g(\delta,\beta)$.

$$g_j(\delta,\beta) = I_j(\delta) - I_j^m \tag{18}$$

Taylor's series expansion gives:

$$(g_j(\delta,\beta)]_{k+1} = [g_1]_k = (\frac{\partial gi}{\partial \delta})_k \Delta\delta + (\frac{\partial gi}{\partial \beta})_k \Delta\beta, \tag{19}$$

where k is the iteration stop number

and $\Delta\delta$, $\Delta\beta$ are corrections to the initial guess.

Since $g_j = 0$ will provide solution, the following set of equations will result:

$$-[g_j]_k = (\frac{\partial gi}{\partial \delta})_k \Delta\delta + (\frac{\partial gi}{\partial \beta})_k \Delta\beta, \tag{20}$$

or in matrix form

$$[D] * (\Delta) = \{G\} \tag{21}$$

System of equations (21) is solved for the unknown increments $\Delta\delta$ and $\Delta\beta$. This process is repeated until the preset convergence limit is achieved.

The main problem with such technique is that the initial guess has to be supplied for procedure to start. If the initial guess is far from actual solution, no convergence is achieved. (The initial guess can be supplied from the above described "Error-summation approach".) One can run it in relatively coarse increments and the obtained approximate solution can be used as an "initial guess".

To verify this approach, several increments were tested for wide range of measured retardation (0-5000nm). It was found, that increment of 40-50nm always provided correct solution with prescribed accuracy.

3.2.4. Discussion of the Data-Acquisition Procedures

All three procedures discussed above eventually gave correct solution for retardation. However, if initial guess in the Newton-Ralpson is relatively far away from the actual solution, the approach does not converge. The following table provides range of initial "guesses" for a particular setup, which does converge:

Table 1

Convergence Range for Newton-Raphson Procedure

Correct Solution (nm)	Permissible Range for Initial guess (nm)
90	50-350
990	690-1255
3000	2800-3200
6990	6700-7200

The solution time was about 2-4 times longer than in the error-summation or data base approaches.

The error-summation approach was always 10-30% faster than data base search approach. As an additional check, the sensitivity of each one of the discussed approaches to errors in data reading was evaluated. The recorded value of light intensity was modified as:

$$I_{new} = (I_{old} + OFF) * FC \qquad (22)$$

where OFF is the offset value

and FC is the scale factor

The following were results obtained by each one of the discussed approaches for a test case of δ = 990nm.

Table 2

Influence of the Measurement Errors on Accuracy of the Results

Offset % of I_{Old}	Factor	Approach		
		Error Summ.	Data Base	Newton-Raphson
30	1.1	930	945	984
	1.3	300	900	334
	1.5	270	120	509
20	1.1	960	240	986
	1.2	945	120	986
	1.3	120	5175	240
10	1.5	945	120	988
	1.9	945	150	988
	2.5	270	5670	3294

Thus, in a wide range of "offset" and "factor" values error-summation and Newton-Raphson approaches were less prone to the introduced error than the data-base approach.

3.2.5. Discussion and Conclusion

Three different procedures were implemented and analyzed for the accuracy and effectiveness in solving the system of 16 equations for unknown retardation. When no error is introduced to this system, all three approaches seem to give similar results, with error-summation being the fastest and most flexible Observation of the Table 2 suggests that data-base search approach is more prone to the errors in light intensity reading. Thus, error-summation technique is the most effective and accurate for extracting the value of retardation from the acquired spectral contents.

Another problem which we expected to encounter was temporal stability of the whole system. The test which we run for four hours by taking readings from the same specimen, exhibiting a permanent residual birefringence did not show any difference in results, illustrating an excellent system stability, for short to medium term.

3.2.6. Software Description

The unknown retardation can be evaluted on the basis of equation (17) as described in section "Methods for Measuring Retardation". The computer program to do this can be described as following:

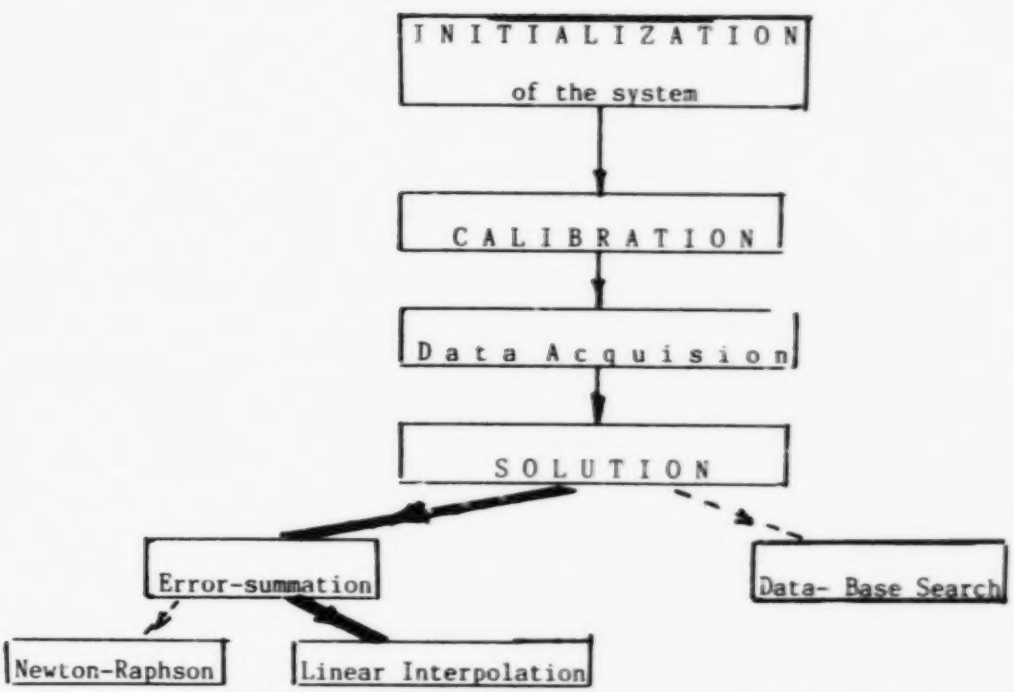

The most desirable pass is shown by a heavy line.

3.2.7. Initialization of the System

The first part of the program assigns all necessary arrays to be used in the process of evaluation of the retardation.

DI(512,16) - Contains theoretical values for light intensities at each one of the 512 values of retardation (0-5120 in 10nm increments) for every one of the 16 available diodes,

DM(16) - Contains actual readings for a given retardation at each one of 16 diodes,

DC(16) - Contains dispertion coefficients for a given material at each one of 16 diodes,

BF(16) - Contains actual readings for a non-stressei specimen in the bright field set-up for each one of 16 diodes,

DF(16) - Contains actual readings for a non-stressed specimen in the dark field set-up for each one of 16 diodes,

E(512) - Values of the error function as calculated in the error-summation part.

3.2.8. Calibration

At this part of the procedure the unstressed specimen is installed in the bright field circular polariscope set-up and resulted light intensity is acquired into array BF(16). Then the set-up is changed into the dark field arrangement and corresponding values of light intensity are acquired into array DF(16). This information is then used to calculate proper values for I (j) for the equation (14).

3.2.9. Data Acquisition

The analog to digital board supplied by METRABYTE is used to acquire analog values of light intensity and convert them in the digital form. Each diode is sampled 64 times and the average value is used in the evaluation procedure. The total time to sample each diode 64 times, convert its value in the digital form and find average values takes less then 1 second for all 16 diodes.

3.2.10. Solution

a. Error-Summation

This part of the program calculates theoretical values DI(512,16) of light intensity as would be seen by each diode at each specified retardation according to equation (15) and compares it to the acquired data (9) as described in section "Error summation approach".

b. Data Base Search

This part is similar to the previous paragraph. The calculated values of the DI(512,16) are compared to the actual ones according to the procedure described in the "Data Base Search".

c. Newton-Raphson

The function g(i) if formed according to (18), all necessary derivatives are calculated as in (19-20) and linear system of equations (21) is solved for a given set of initial values of the unknowns. The solution is used as an input value for the next iteration. This process is repeated until necessary convergence is achieved.

d. Linear Interpolation

To increase the accuracy of the results in the "Error summation approach" simple technique of linear interpolation is used. The interval of 10nm less and more than the calculated value of retardation is divided into smaller subdivisions (i.e., 1nm) and process of error summation is repeated for this range.

3.3. Evaluation of Materials

3.3.1. All transparent materials develop birefringence when stressed. Consequently, the SPECTRAL CONTENTS ANALYSIS is not restricted to any specific material, and can be used in Q.C. operations of any transparent or translucent item.

When chosing a birefringent material for a sensor, one should examine a variety of materials and determine the most suitable candidate. In this research project three materials were evaluated:

a) Polycarbonate

This material exhibits a very high strain-optic constant k. It is stable up to temperature of 275°F and the creep is negligible making this material suitable for an optical sensing element operating below 275°F.

b) Epoxy Resin

This material is easily castable to any desired shape and exhibits a high strain-optic response. It is used extensively in the photoelastic stress analysis.

c) Glasses

Glass in various grades and composition can be selected for a birefringent sensing element, or a fiber-optic birefringent sensor. The advantages of the glass sensor are:

- High Brewster Constant (typically 3.0)
- Low coefficient of thermal expansion
- Capability of elevated temperatures

In addition to ordinary glass, the potential sensor materials should include fused silica, or semi-conductor materials (silicon or germanium) that are useful in the infrared range.

3.3.2. Dispersion of Birefringence

The Brewster Law (equation 2 above) expresses that the measured retardation δ is proportional to stresses:

$$\delta = tC(\sigma_1 - \sigma_2)$$

The material constant C is slightly wavelength dependent, and must be evaluated, in order to accurately implement the SPECTRAL CONTENTS ANALYSIS. It was experimentally verified that for some materials C is nearly constant, but other materials (4)(5) C is variable and these variations must be included in the computation as shown in the equations (12) above.

In the research carried, the constant C was measured within the visible spectrum and the results of these measurements are shown in Figure 9.

For polycarbonate, C increases significantly at the blue end of the spectrum. To account for the variations of C, one can rewrite the transmitted light intensity as follows:

$$T_M(\delta,\lambda) = \text{Sin}^2 \frac{\pi\delta_\lambda}{\lambda}$$

In this equation, δ is not independent of the wavelength λ, but δ/C is wavelength independent. Selecting a central region of the visible spectrum as a standard (or reference) λ_o = 570nm and C_o as a normalized value, we can write:

$$\delta_\lambda = \delta_o \frac{C(\lambda)}{C_o}$$

and the transmittance equation becomes:($C = C(\lambda)$)

$$T_M(\delta,\lambda) = \text{Sin}^2 \frac{\pi\delta_o}{\lambda} \cdot \frac{C}{C_o}$$

where C/C_o becomes a correction factor accounting for the chromatic dispersion of the birefringence.

The value of the chromatic dispersion coefficient C/C_o can be stored for all the wavelength used in the array and the needed correction applied within the programs software.

3.4. Analysis of the Quarter-Wave Plate Behavior in a White Light Polariscope

A quarter-wave plate is a birefringent exhibiting a uniform retardation of $\frac{1}{4}$ wavelength throughout its area. In monochromatic light, the quarter-wave plate is selected in accordance with the monochromatic light used. In white light employing a broad spectrum of wavelength, the quarter-wave plate is only approximating the ideal $\frac{1}{4}$ wavelength retardation for most radiations.

If λ_o is a nominal wavelength within the spectral range selected, the retardation of the quarter-wave plate for this radiation is:

$$\delta = \lambda o/4$$

and the corresponding phase shift is $\pi/2$ at λ_o. For other wavelength values λo the phase angle is $2\pi \frac{\delta o}{\lambda}$ and the error of the quarter-wave plate becomes:

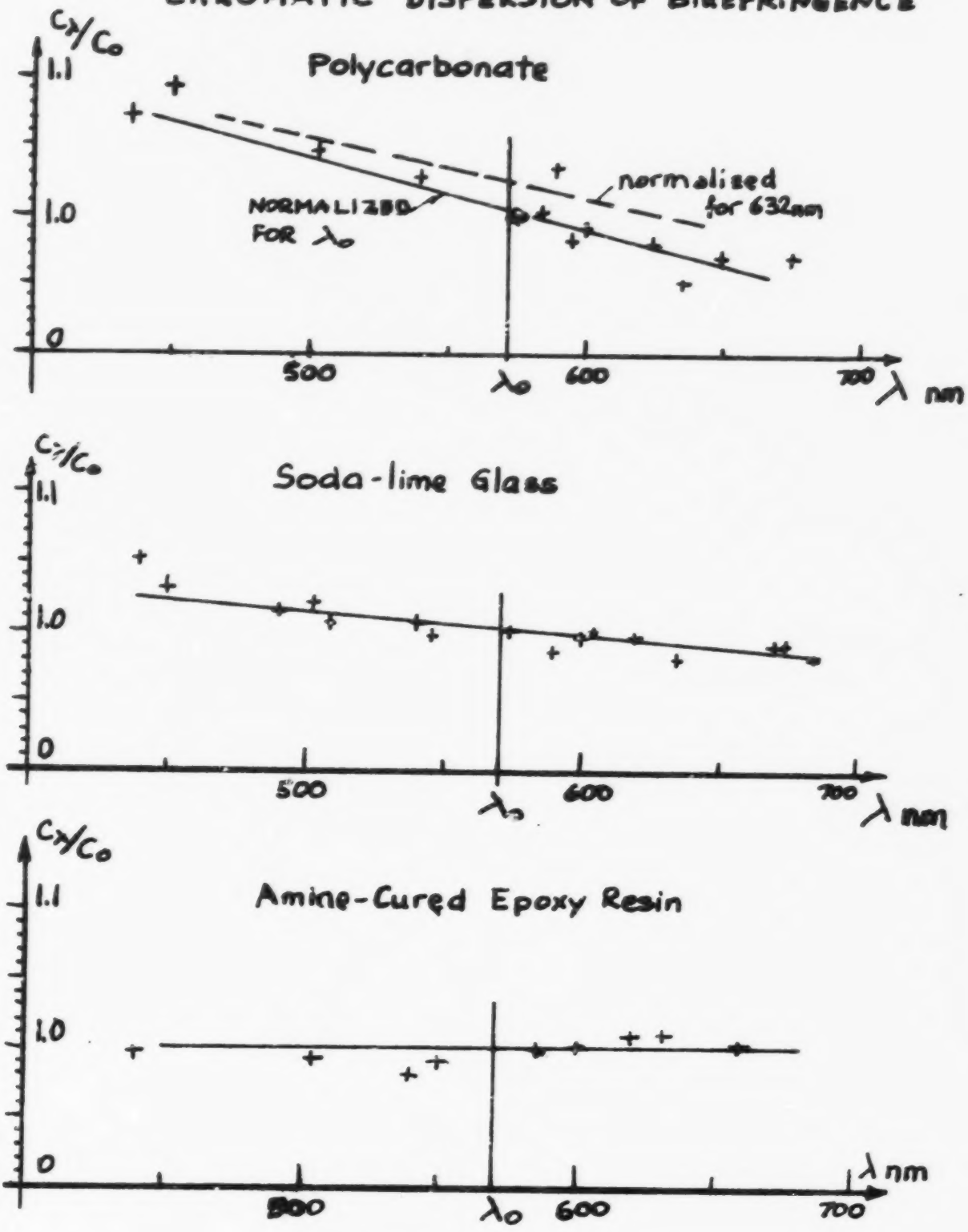
CHROMATIC DISPERSION OF BIREFRINGENCE
Cλ/Co
Polycarbonate
1.1
1.0
0
NORMALIZED FOR λo
normalised for 632nm
500
λo
600
700
λ nm
Cλ/Co
Soda-lime Glass
1.1
1.0
0
500
λo
600
700
λ nm
Cλ/Co
Amine-Cured Epoxy Resin
1.1
1.0
0
500
λo
600
700
λ nm

FIGURE 9

$$e = \frac{\pi}{2}\left(\frac{\lambda o}{\lambda} - 1\right)$$

This "error" will affect the transmitted light intensity, and in some instances, it could be incorporated in the program, to reduce the potential measurement error. The light intensity transmitted by a system containing the quarter-wave plate error was derived as shown in the Appendix 1 and the resulting transmittance is:

$$T_M(\delta,\lambda) = \mathrm{Sin}^2 \frac{\pi\delta}{\lambda}(1-\mathrm{Sin}^2 2\alpha \mathrm{Sin}^2 2e)$$

The term in parentheses represents the influence of the quarter-wave plate error e.

The influence is most significant when the principal stresses in the observed element are at 45° to the quarter-wave plate axes. The error is completely eliminated when the quarter-wave plate axes are aligned with the stressed element. Several possible approaches can be suggested, for a system set-up depending upon the system functions:

a) When the direction of principal stress is known the error is completely eliminated. (In this case, the quarter-wave plates can be completely eliminated.)

b) When the direction α between the stress and the quarter-wave plate is variable, one can minimize the error setting the $\mathrm{Sin}^2 2\alpha = 0.5$.

c) The most effective way to eliminate the potential error is to incorporate in the program a two-step solution. In the first search, a broad spectral image is used, to locate approximately the value of the searched δ. At this state, the spectral range would be approximately 300nm. For the final search, a narrower band (approximately 150nm) can be used, minimizing the error:

$$e = \frac{\pi}{2}\left(\frac{600\pm75}{600} - 1\right) = \pm.125\times\frac{\pi}{2}$$

The resulting light intensity error is only 2%. Without these precautions, the error could become 14%, which is not negligible.

The experiments that were carried out confirmed the above conclusions, although the influence of the light intensity error on the measured birefringence seemed insignificant.

3.5 Problems Associated with the Selection of Spectral Range and the Choice of Photodiodes Spacing

Using the wide range of wavelength, several problems discussed above must be dealt with, and resolved:

a) The commercial polarizers are efficient only in a very narrow range.

b) The quarter-wave plate is further restricting the range of wavelength.

c) The material chromatic dispersion can become significant in a broad range.

The SPECTRAL WIDTH should, therefore, be restricted to a minimum compatible with the need of obtaining a reliable solution. A narrow spectral width creates secondary minima of the error function, that could produce an erroneous readout if the steps of the search are larger than the width of the minimum spike (see Figure 10).

Combining the above requirements, it appears that a spectral range of 250 to 350nm should be satisfactory for most applications.

Another important design parameter affecting:

a) The speed of the processing

b) The precision

c) The max. range of measurable retardation, is the number of the photodiodes and their spectral resolution.

In our experiment, a specimen subjected to a constant stress was measured using:

a) 16 photodiodes, over a 320nm range

b) 8 photodiodes over a 320nm range

c) 8 photodiodes over a 160nm range

The results were somewhat suprising: In all instances, the "δ" measured by the SPECTRAL CONTENTS ANALYZER was the same, demonstrating that 8 photodiodes are sufficient, within the range of 0-5000nm that was evaluated.

A larger number of photodiodes could become useful when the range is expanded beyond 5000 PROVIDED a higher dispersion grating is used to narrow down the band-width of each individual photodiode.

3.6. Use of Fiber-Optic Cables for Data Acquisition in the SPECTRACL CONTENTS ANALYSIS

The use of fiber-optic cables increases the usefulness of the birefringent sensor, since the information can be transmitted easily, remote readout is possible, multi-point data acquisition using one central spectral analyzer can be easily implemented. The system was tested with and without the fiber-optic cable. The performance was nearly identical, in fact, the instrumentation was easier to set-up and operate.

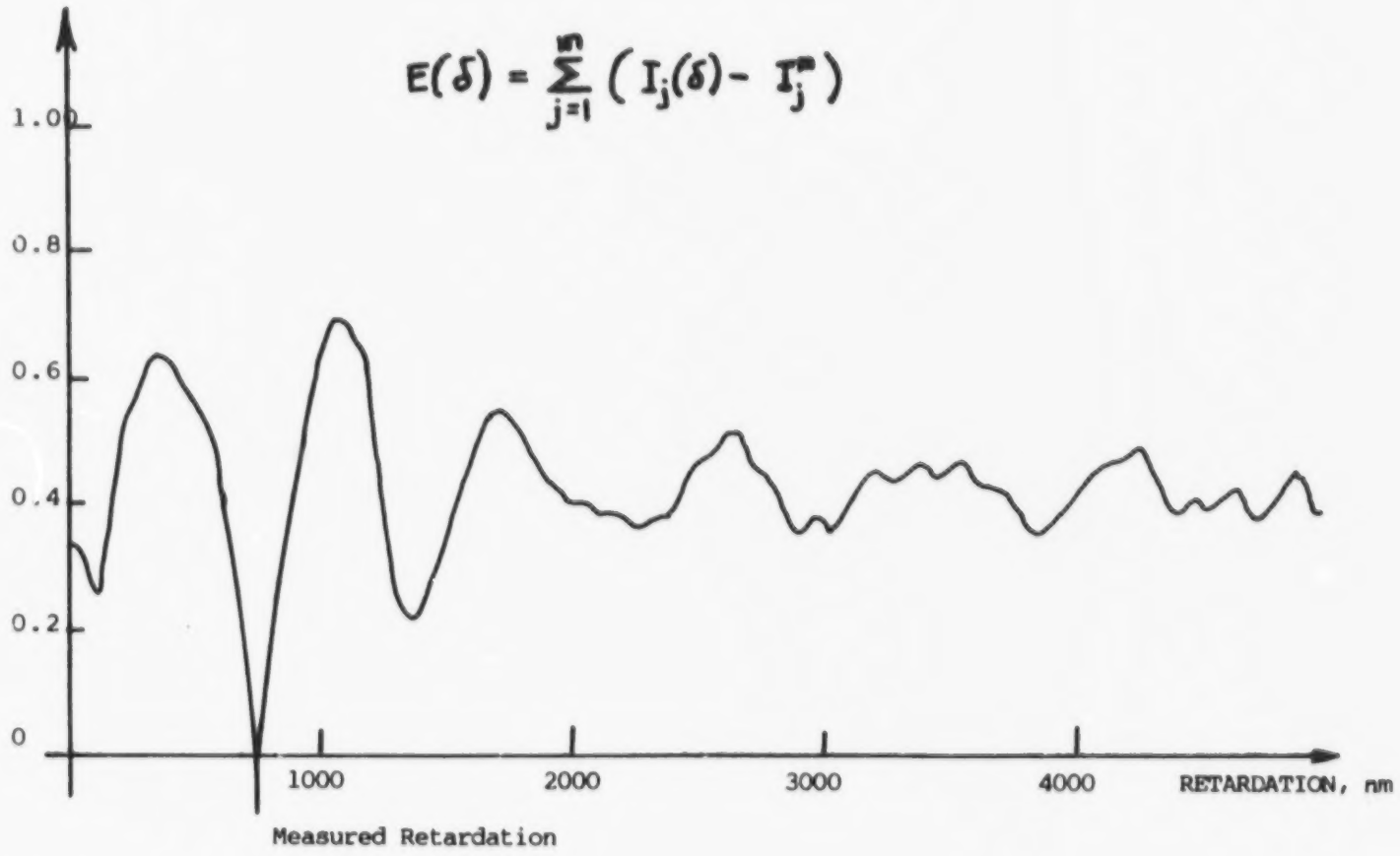

FIGURE 10. Error Function Used in the Search For the Measured Retardation

POLYCARBONATE (A= 41x6.35 mm)			
FORCE N	STRESS kPa	MEASURED RETARD. nm	
0	0	10	24
111	427	220	236
222	854	420	444
334	1,281	660	676
445	1,709	890	902
556	2,136	1,112	1,130
667	2,563	1,356	1,366
778	2,990	1,566	1,576
890	3,417	1,796	1,814
1,001	3,844	2,002	2,010
1,112	4,272	2,222	2,230
1,223	4,698	2,452	

AMINE-CURED EPOXY (A= 25x3.1mm)			
0	0	10*	10**
111	1,435	250	250
222	2,870	470	470
334	4,306	730	730
445	5,740	950	950
556	7,175	1,180	1,180
667	8,610	1,440	1,440

* 16-Photodiode Array
** 8-Photodiode Array

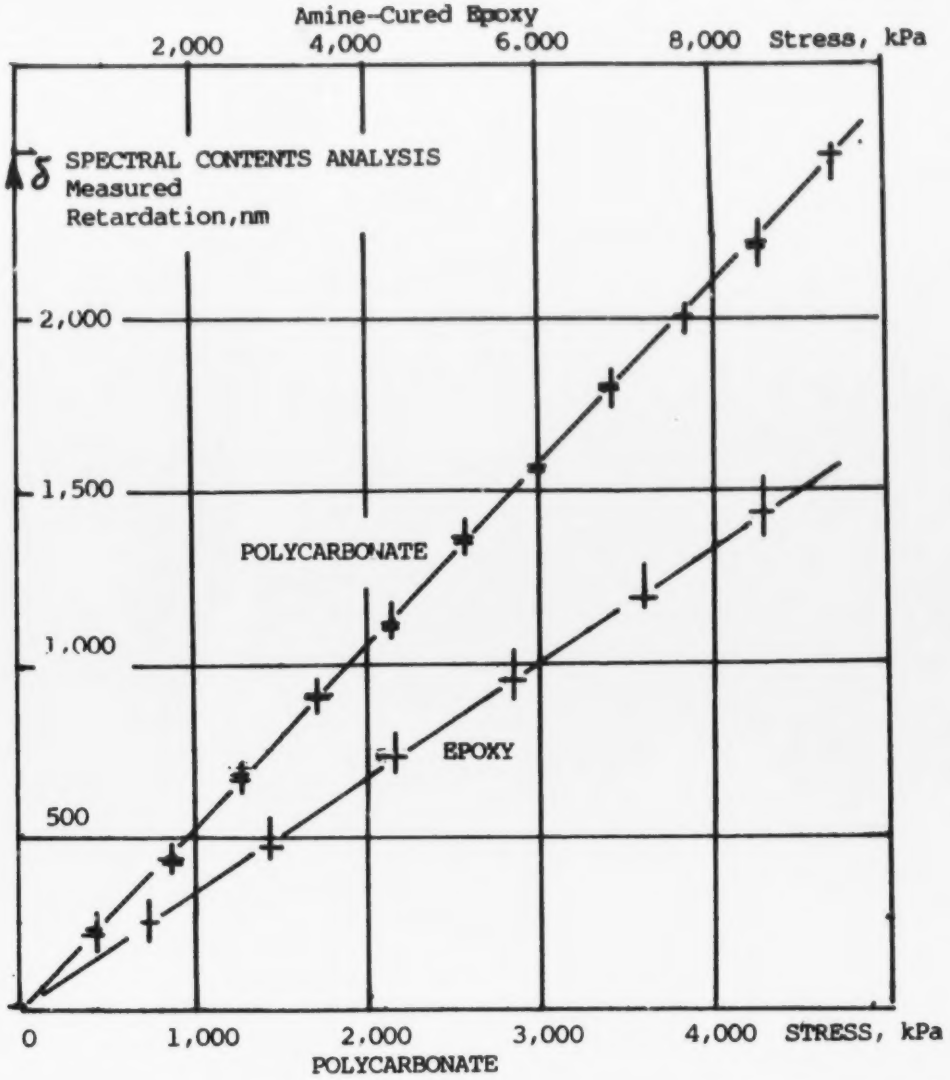

FIGURE 11. TENSILE TEST RESULTS.

3.7 System Evaluation

Upon completion of the system shown schematically on the Figure 2 and in its finished form on the Figure 7, the testing and evaluation was performed as follows.

3.7.1. Measuring of Stress-Induced Birefringence

Tensile beams 38mm wide 6.35mm thick and 250mm long ($1\frac{1}{2}$"X$\frac{1}{4}$"X10") were placed in a testing frame (Photolastic Model 082) equipped with an electric resistance strain gage load cell and load cell readout Model 082B. Two polycarbonate beams and one amine-cured epoxy beam were tested, subjecting each one to an increasing load. The retardation was measured first using a conventional polariscope and then using Spectral Analysis System. The results of these measurements are shown on the Figure 11.

The retardation-versus-force plot shows an excellent linearity. Particular attention was paid to the retardation 0-2500nm range that represents the most frequently used range of photoelastic measurements.

3.7.2. Measuring of Permanent Birefringence

In order to evaluate the ability of the method to measure residual stresses and also to assess the precision of measurements, the following additional measurements were performed.

Measurements of High Retardation Values

Constant retardation plate exhibiting retardation of 4.5 wavelength and 2.1 wavelength were inserted individually and then in series, producing a total retardation of 6.6 wavelength, or approximately 3800nm. The SPECTRAL CONTENTS ANALYZER resolved this retardation, providing repeatable reading. The retardation plate was consequently related in its own plane, changing the angle α between the direction of principal stresses and quarter-wave plates axes. This rotation did not produce a change in the indicated retardation, proving an important characteristic of the system and demonstrating that the retardation CAN BE MEASURED independently of the direction of principal stresses.

Evaluation of Precision

A polycarbonate plate 75mmX75mmX6.35mm thick exhibiting a permanent birefringence was used for evaluation. This specimen was used during a round-robin study to determine the precision of the ASTM test method D4093, using a compensator for measuring retardation.

The range of retardation measured by five laboratories in this round-robin program was between 700 and 855nm, with average 766nm. The measurement by the SPECTRAL CONTENTS ANALYZER yielded 770nm, which is in good agreement with the data of the round-robin and corroborates the accuracy of the system.

3.7.3. Results

The results of the system evaluation proved that the precision of the system exceeded our most optimistic expectation, leaving no doubt about the feasibility of the method and its potential.

4.0. SUMMARY OF THE RESULTS

As result of this program ALL the research objectives were successfully attained and the following results were made available:

- A special apparatus for Spectral Contents Analysis was developed, designed, completed in a very short time and is now operational, in a form of a research prototype.

- Several algorithms were tested, to assess their suitability, convergence and speed of operation. The most suitable solution was implemented and evaluated.

- The performance of Polycarbonate, Amine-Cured epoxy and glass was evaluated in the SPECTRAL CONTENTS SYSTEM, as a sensor. Since the dispersion of birefringence was found to be influential, the dispersion was measured.

- An extensive analysis was carried to analytically evaluate the performance of quarter-wave plate. The expressions that were developed are needed to introduce the corrective terms in the equations used to express the light intensity.

-A fiber-optic cable was introduced, as an integral part of the birefringence measuring system.

5.0. ESTIMATES OF THE TECHNICAL FEASIBILITY

The results of the research work amply demonstrated that the MEASUREMENT OF BIREFRINGENCE, STRAIN or STRESS on a transparent sensor-material is:

- FEASIBLE, AND RELATIVELY EASY TO ACCOMPLISH

5.1. Instrumentation

The instrument designed for the implementation of the SPECTRAL CONTENTS ANALYSIS is a simplified spectrophotometer using 8 to 16 wavelengths, and can be produced from standard components.

5.2. Materials

Material exhibiting a desired mechanical or temperature behavior can be used as birefringent sensor. A potential candidate for high-temperature should include:

Fused Silica (max temp. 1000°C)

Sapphire (max temp. 1,500°C)

Zerodur (low thermal expansion)

5.3 Precision Evaluation

The precision was evaluated comparing the retardation measured using the SPECTRAL CONTENTS ANALYSIS to the retardation measured by classical means, using a compensator.

The specimen selected for the evaluation of the precision was a 75mmX75mm(3"X3") clear polycarbonate 6.35mm thick (¼'in) that was exhibiting a uniform birefringence due to the residual strains acquired in the manufacturing process. This material was used previously for evaluation of the precision of the ASTM D4093 test method, in a Round-Robin study in which five laboratories participated, establishing the precision and bias statement. The retardation measured visually using a compensator (2) yielded a retardation δ ranging from 700nm to 855nm, with each laboratory reporting data ±40nm, and an interlaboratories ave. 766 nm.

The specimen inserted in the SPECTRAL CONTENTS ANALYSIS provided a consistent and reproducible reading δ = 770nm.

The sensitivity was selected arbitrarily to be 10nm, and was designed into the program. As result of the research it appears that the potential precision is BETTER than the ±10nm.

5.4 Potential Applications

The potential applications of the techniques that were developed as result of this research program are:

5.4.1. Photoelastic Measurements

Using the SPECTRAL CONTENTS ANALYSIS - a totally automated, microcomputer controlled data acquisition system for 2 and 3-dimensional model analysis and a similar instrument for photoelastic coating can be produced, eliminating long hours of visual anlaysis and providing accurate data, free of human errors.

5.4.2. Birefringent Sensors

A properly selected transparent material can be used as a BIREFRINGENT SENSOR. A FIBER-OPTIC BIREFRINGENT STRAIN SENSOR can be used similarly to a strain gage, using the SPECTRAL ANALYZER developed as the result of this research to retrieve the strain, or any other measured quantity.

5.4.3. High Temperature Capabilities

Using fused silica as a sensor material, a high-temperature strain sensor or transducer can be designed, and data received using the methods developed.

5.4.4. Process Controls

At the present time, there is no suitable method to control the FLOAT GLASS process, plastic sheet extrusion or plastic film orientation.

The technique developed as result of this research will permit IN LINE data acquisition, transmission of data by means of fiber-optic cables to a process-control room and remote readout of strains at any desired number of points.

5.4.5. Non-Destructive Testing and Q.C. of Glass and Plastic Products

Presently used methods are slow and expensive to implement. The SPECTRAL CONTENTS ANALYSIS can replace a subjective visual evaluation by a reliable, self-operated readout, permitting a 100% inspection, elimination of defective materials and decrease in inspection costs.

6.0 CONCLUSIONS AND RECOMMENDATIONS

From the results of this research the following conclusion can be reached:

- The proposed SPECTRAL CONTENTS READOUTS method of data acquisition for birefringent sensor is:

- MORE ACCURATE THAN PRESENTLY KNOWN APPROACHES
- TECHNICALLY FEASIBLE AND ECONOMICALLY ADVANTAGEOUS
- APPLICABLE TO MANY PRACTICAL COMMERCIAL APPLICATIONS

Recommendations

The research performed solved most of fundamental problems, related to the algorithms, handling of the equations, and spectral region requirements. To IMPLEMENT this technology, and take full advantage of its economical and technical features, it will be necessary to develop a "commercial" system incorporating all the knowledge gained. In such an industrial design the PC microcomputer will be replaced by an on-board microprocessor, the research-type polarimeter design by an industrial-probe type of head, and the light source reduced in size to a miniature bulb powered by a rechargeable battery. In addition to the hardware, SOFTWARE for the system operation will be needed, tested and debugged, to permit the operation by non-technical personnel.

Additional research will also be needed to test the proposed system at ELEVATED TEMPERATURE and develop fiber-optic general-purpose strain sensors and strain gage.

Funding for continuation of this project to insure the implementation and development of a useful product(s) will be solicited in the PHASE II of SBIR program and from industrial investors, including potential commercial users.

REFERENCES

1. ASTM F218-83 "Analyzing Stress in Glass" ASTM Books of Standards, 1916 Race St., Phila., PA (published yearly).

2. ASTM D4093-85 "Photoelastic Measurements of Birefringence and Residual Strains in Transparent or Translucent Plastic Materials" ASTM Books of Standards, 1916 Race St., Phila., PA (published yearly).

3. Redner, A.S. "Photoelastic Measurements by Means of Computer-Assisted Spectral-Contents Analysis" Experimental Mechanics 25(2) pp 148-153, June 1985.

4. Redner, A.S. "Photoelastic Data Acquisition in Infrared" VDI Berichte No 313, pp 57-62 (1978).

5. Pindera, J.T. and Cloud, G. "On Dispersion of Birefringence of Photoelastic Materials" Experimental Mechanics 6(9) pp 470-480 (1966).

6. Sanford, R.J. and Iyengar, V. "The Measurement of the Complete Photoelastic Fringe Order using a Spectral Scanner" Procedings SEM, Las Vegas, Nevada (1985).

7. Research Report D-20#1121 Jan 22, 1985 filed with ASTM, 1916 Race St., Phila., PA.

APPENDIX

Derivation of the Transmitted Light Intensity. Circular Polariscope with Quarter-Wave plate retardation $\lambda o/4$ operating in white light.

The figure below illustrates the angular position of all elements, arranged in accordance with the Figure 1 (Dark or Light Field) set-ups.

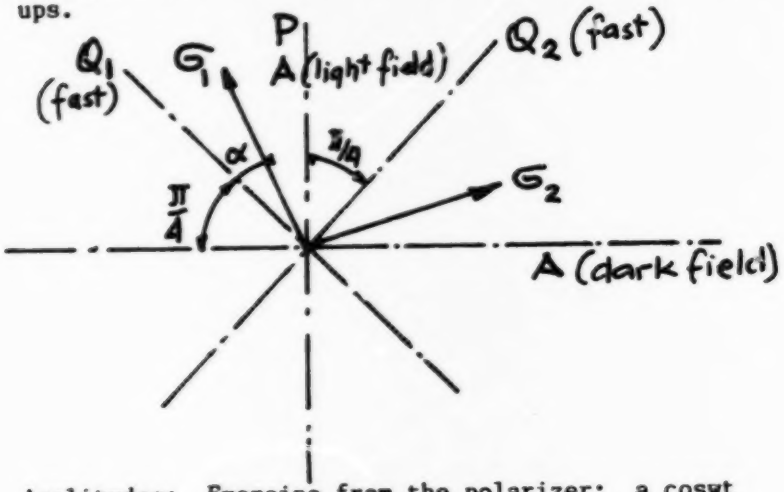

Amplitudes: Emerging from the polarizer: a coswt

Emerging Q_1: F(Fast Axis) $a \cdot \frac{\sqrt{2}}{2}$ Sin(wt+ε)

S(Slow Axis) $a \cdot \frac{\sqrt{2}}{2}$ Cos(wt-ε)

where ε is the phase error of the quarter-wave plate. Projecting the "F" and "S" components on the principal axes σ_1 and σ_2 of the stressed material, we have:

$(on\ \sigma_1)$: (Fcosα + SSinα)

$(on\ \sigma_2)$: (-FSinα + SCosα)

the retardation δ in the stressed material introduces a relative shift

$\varphi = \frac{2\pi\delta}{\lambda}$

The components <u>emerging</u> from the birefringent plate are:

$(on\ \sigma_1)$: $\frac{a\sqrt{2}}{2}[\cos\alpha\ \mathrm{Sin}(wt+\varepsilon-\varphi) + \mathrm{Sin}\alpha\ \mathrm{Cos}(wt-\varepsilon-\varphi)]$

$(on\ \sigma_2)$: $\frac{a\sqrt{2}}{2}[-\mathrm{Sin}\alpha\ \mathrm{Sin}(wt+\varepsilon) + \mathrm{Cos}\alpha\ \mathrm{Cos}(wt-\varepsilon)]$

These components are projected on the Q_2 axes. Entering Q_2 we have:

$$F(Q_2): \quad \sigma_1 \sin\alpha + \sigma_2 \cos\alpha$$

$$S(Q_2): \quad -\sigma_1 \cos\alpha + \sigma_2 \sin\alpha$$

Assuming that the Q_2 quarter-wave plate produces the same retardation as Q_1 and contains the same error $\pm\varepsilon$, emerging from Q_2 we have:

$$F(Q_2) = \frac{a\sqrt{2}}{2}[-\sin\alpha\cos\alpha\cos(wt+2\varepsilon-\varphi) + \sin^2\alpha\sin(wt-\varphi) + \sin\alpha\cos\alpha\cos(wt+2\varepsilon) + \cos^2\alpha\sin wt]$$

$$S(Q_2) = \frac{a\sqrt{2}}{2}[-\cos^2\alpha\sin(wt-\varphi) - \sin\alpha\cos\alpha\cos(wt-2\varepsilon-\varphi) - \sin^2\alpha\sin wt + \sin\alpha\cos\alpha\cos(wt-2\varepsilon)]$$

The amplitude transmitted (projected on) the analyzer in a dark field setting becomes:

$$\frac{\sqrt{2}}{2}(F + S)$$

and the light intensity (square of the amplitude) becomes:

$$I = \sin^2 \frac{\pi\delta}{\lambda}[1-\sin^2 2\alpha \sin^2 e]$$

In light field setting the amplitude is:

$$\frac{V2}{2}(F-S)$$

and the light intensity becomes: $I = \cos^2\frac{\pi\delta}{\lambda} + \sin^2\frac{\eta\delta}{\lambda}\sin^2 2\alpha\sin^2 e$

NASA National Aeronautics and Space Administration

Report Documentation Page

1. Report No.	2. Government Accession No.	3. Recipient's Catalog No.
NASA CR-179430		

4. Title and Subtitle	5. Report Date
SPECTRAL CONTENTS READOUT OF BIREFRINGENT SENSORS	April 1988
	6. Performing Organization Code

7. Author(s)	8. Performing Organization Report No.
Alex S. Redner and Dr. Arkady S. Voloshin	H-1444
	10. Work Unit No.
	RTOP 505-63-31

9. Performing Organization Name and Address	11. Contract or Grant No.
Strainoptic Technologies, Inc. P.O. Box 177 Norristown, Pennsylvania	NAS2-12351
	13. Type of Report and Period Covered
	Contractor Report - Final

12. Sponsoring Agency Name and Address	14. Sponsoring Agency Code
National Aeronautics and Space Adminstration Washington, DC 20546	

15. Supplementary Notes

NASA Technical Monitor: Alan L. Carter, Ames Research Center, Dryden Flight Research Facility, Edwards, California 93523-5000

16. Abstract

The objective of the research work performed was to establish the feasibility of using SPECTRAL CONTENTS ANALYSIS to measure accurately, strains and retardation in BIREFRINGENT SENSORS, and more generally, on transparent materials.

17. Key Words (Suggested by Author(s))	18. Distribution Statement
Photocell Spectral Analysis Photoelasticity Spectral Analysis Spectrometer	Unclassified - Unlimited Subject Category 39

19. Security Classif. (of this report)	20. Security Classif. (of this page)	21. No. of pages	22. Price
Unclassified	Unclassified	38	A03

NASA FORM 1626 OCT 86